Progress Toward Understanding Injection Timing Sensitivity with Stepped-Lip Diesel Piston Bowls

SAND2018-0835PE

Steve Busch, Kan Zha
Sandia National Laboratories
Federico Perini, Rolf Reitz
University of Wisconsin-Madison

January 30, 2018

Previous research on turbulent flow structure evolution with stepped-lip pistons suggests that rapid mixing is associated with the formation of recirculating flow patterns in the squish region and above the step. Increased mixing rates lead to faster, more efficient combustion, and may enhance soot oxidation processes. These recirculation flow patterns do not form for main injection timings near top-dead-center (TDC), which may limit efficiency benefits of stepped-lip pistons. The objective of this work is to understand the mechanism responsible for the changes in turbulent flow structure as injection timing is advanced toward TDC. Fuel splitting changes dramatically with injection timing, and more fuel mass and momentum are deflected upward at the outer bowl rim for injection timings approximately 10 crank angle degrees (CAD) after TDC, when the piston is positioned several millimeters below its TDC position. Bulk gas density decreases as the cylinder contents expand, which decreases air entrainment into the injection jets and increases their penetration velocity. As a result, jet-wall interactions occur sooner when the main injection starts at approximately 10 CAD after TDC; the continued delivery of fuel mass and momentum during the injection continues to drive the upward deflection of the jets. Vertical gradients of radial velocity above the outer bowl rim increase significantly in magnitude as injection timing is retarded; these gradients drive outward radial acceleration that is expected to promote the formation of beneficial recirculating flow patterns in the squish region.

Sandia National Laboratories is a multimission laboratory managed and operated by National Technology and Engineering Solutions of Sandia, LLC., a wholly owned subsidiary of Honeywell International, Inc., for the U.S. Department of Energy's National Nuclear Security Administration under contract DE-NA0003525.

Advantages of stepped-lip pistons and implications for improving diesel engine efficiency

- Two advantages of stepped-lip pistons (compared to conventional re-entrant pistons)
  - Faster mixing controlled combustion – linked to appearance of recirculating flow structures (not well understood)
  - Decreased soot emissions through improved air utilization

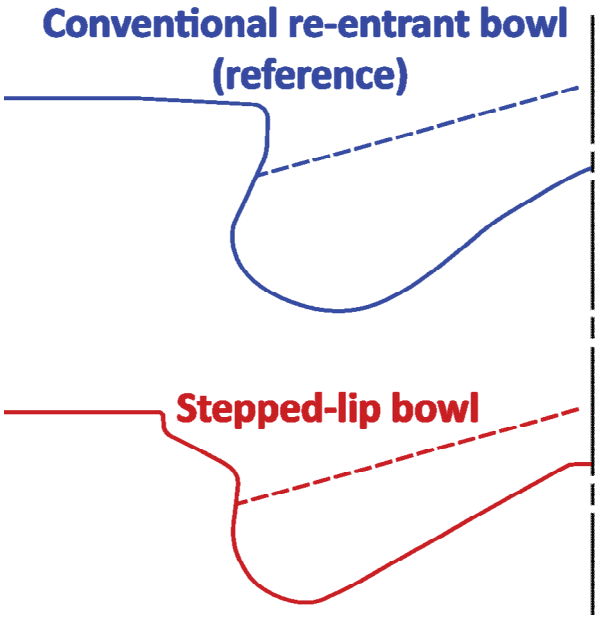

- Pathway to improved efficiency
  - Better air utilization → increased EGR tolerance
  - Higher EGR rates → decrease NOx emissions
  - Lower NOx emissions → more advanced combustion timing possible
  - More advanced combustion timing → improved thermal efficiency

Limits to efficiency improvement mechanism with stepped-lip piston

- Experimental data from SNL small-bore diesel engine
  - 1500 rpm, 9 bar IMEPg
  - Pilot-main injection strategy
  - Sweep injection timing
- Efficiency gains decrease as injection timing is advanced
- Soot emissions improvements decrease at advanced injection timings
- Objective: understand the mechanism responsible for diminishing benefits with stepped-lip pistons at advanced injection timings

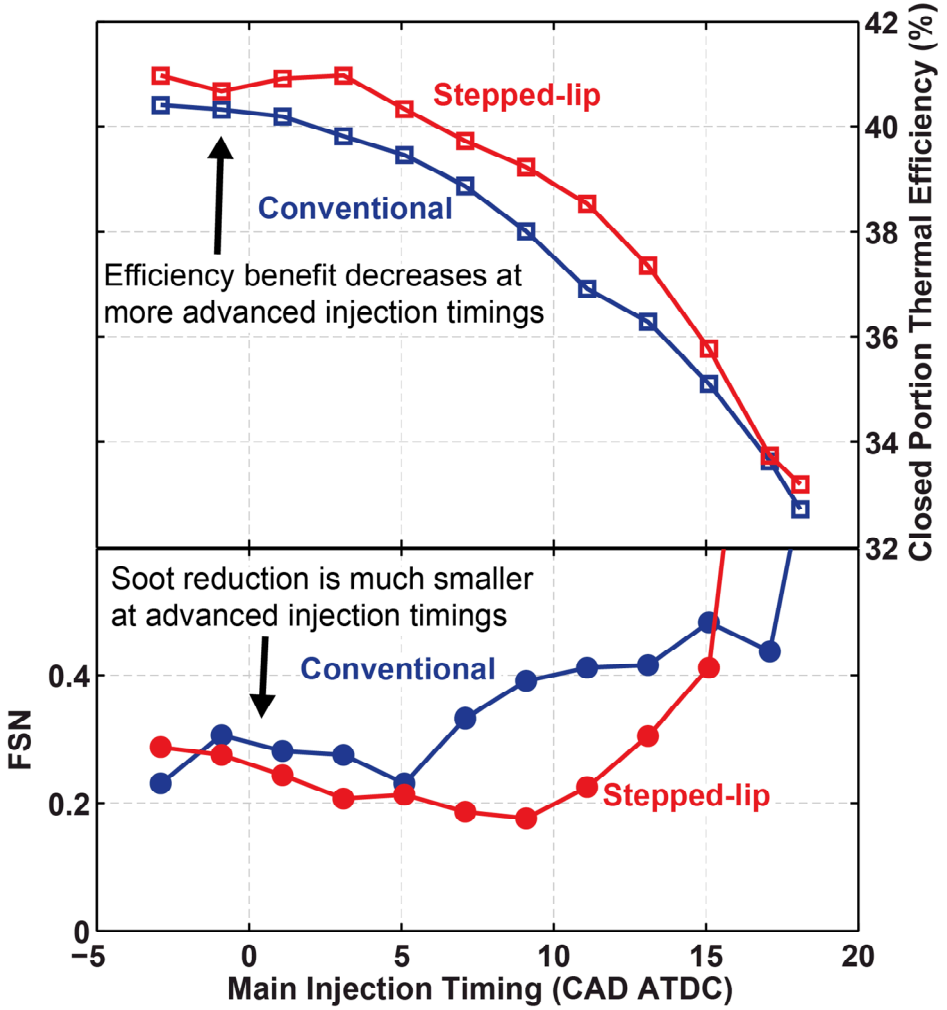

Outline

- CFD simulations using FFRESCO
  - Operating conditions, CFD setup (FRESCO)
- Results/discussion
  - Factors that influence turbulent flow evolution near and in the squish region
- Summary
- Next steps in this project

CFD simulation boundary conditions

- Previous presentations have focused on two piston geometries and three injection timings
- Today's focus is on conventional diesel combustion with the stepped-lip piston and two injection timings
  - "Near-TDC": main injection starts shortly before TDC
  - "Intermediate": main injection starts 10 CAD later

Engine speed	1500 rpm
$IMEP_g$	9.0 bar
Rail pressure	800 bar
m_{pilot}	1.4 mg/str
Pilot-main dwell	1200 µs
SOI_{main}	0.9 CAD BTDC: "Near-TDC" 9.1 CAD ATDC: "Intermediate"
P_{intake}	150 kPa abs
T_{intake}	353 K
T_{TDC}	925 K (est.)
TDC density	21.8 kg/m³
EGR	7% (10.3% accounting for residual fraction)
$[O_2]_{intake}$	19.73%
Fuel	DPRF58 (CN 50.7) 58 vol% Heptamethylnonane 42 vol% n-Hexadecane

FRESCO simulation setup

Engine configuration	
Compression ratio	16.1 : 1
Squish height at TDC [mm]	1.36
Operating conditions	
Engine speed [rev/min]	1500
Intake pressure [bar]	1.5
Intake temperature [K]	353
Injection pressure [bar]	800
Swirl Ratio (Ricardo) [-]	2.2
Intake charge [mol fr.]	0% O_2
FRESCO solver setup	
mesh type:	Body-fitted, unstructured hexahedral mesh
time accuracy:	hybrid 1st-order implicit (diffusion, momentum) / explicit (advection)
spatial accuracy:	2nd-order (diffusion) upwind (advection)

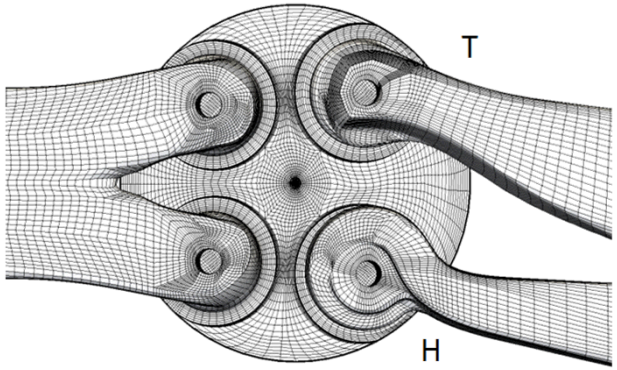

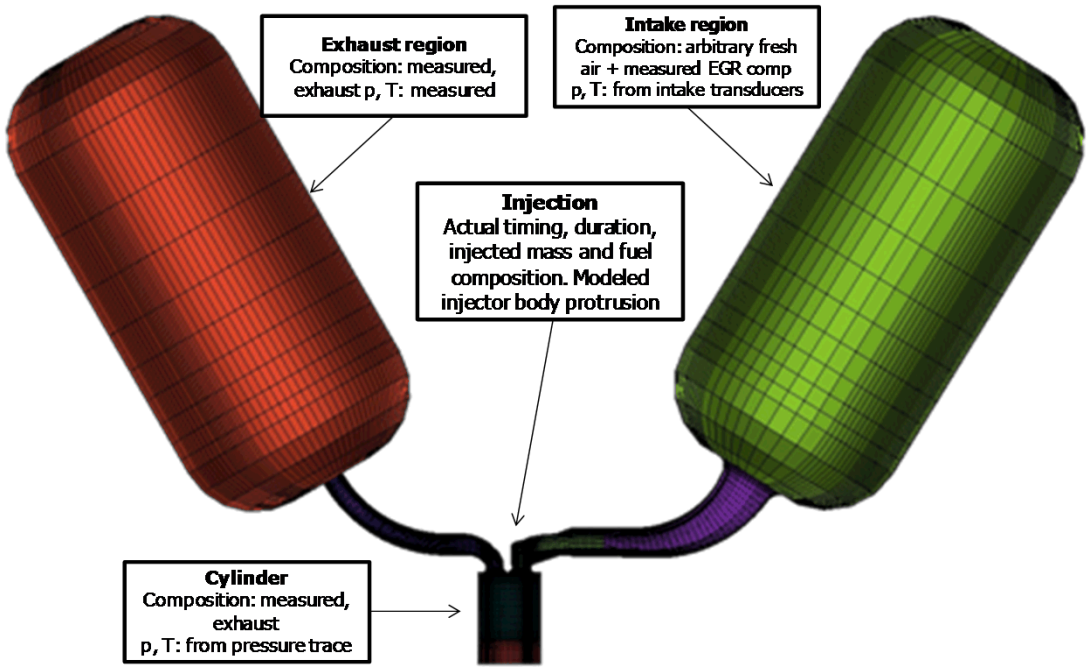

Factors that may influence flow evolution in and around the squish region as injection timing changes

- Spray targeting / fuel splitting
  - Changing mass and momentum delivery out of the piston bowl
- Reverse squish flow
  - Decays during the expansion stroke
- Charge density
  - Change in air entrainment, jet spreading, penetration velocity
- Pressure gradients in the squish region
  - May impede penetration to differing degrees as injection timing changes
- Convection of momentum

Injection timing affects spray targeting evolution

- Near-TDC injection timing
  - Spray targeting is essentially static during main injection
  - Injector axes intersect piston below inner rim
- Intermediate injection timing
  - Piston moves down throughout injection
  - Spray is targeted at the chamfered step surface during the main injection

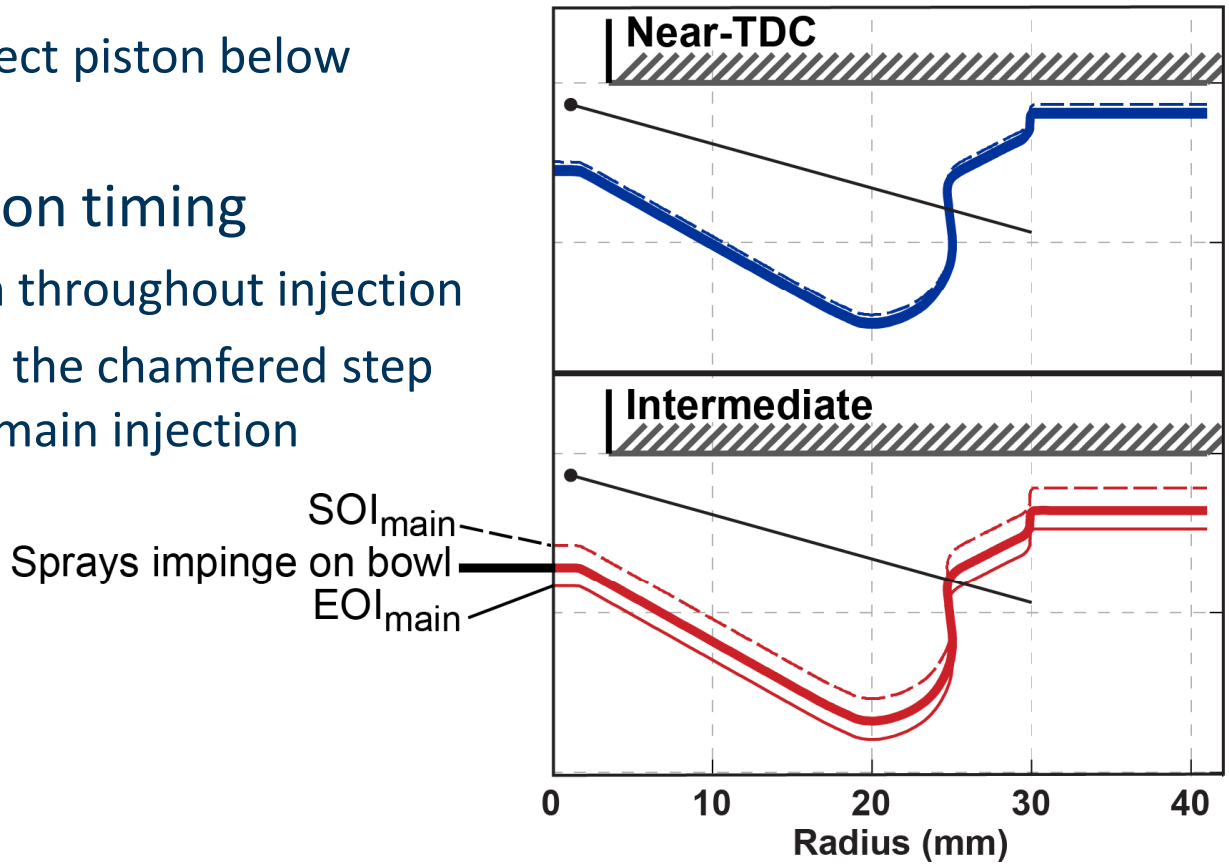

Spray targeting affects fuel mass distribution

- Portion of fuel mass found above the jet axes increases with time for the intermediate main injection (bottom left plot)
  - These results are largely consistent with expectations based on spray targeting
- Fuel mass distribution does not follow the same trend as the volume ratio (bottom right plot)
  - Fuel distribution is not determined solely by availability of volume; spray-wall interactions must also play a role

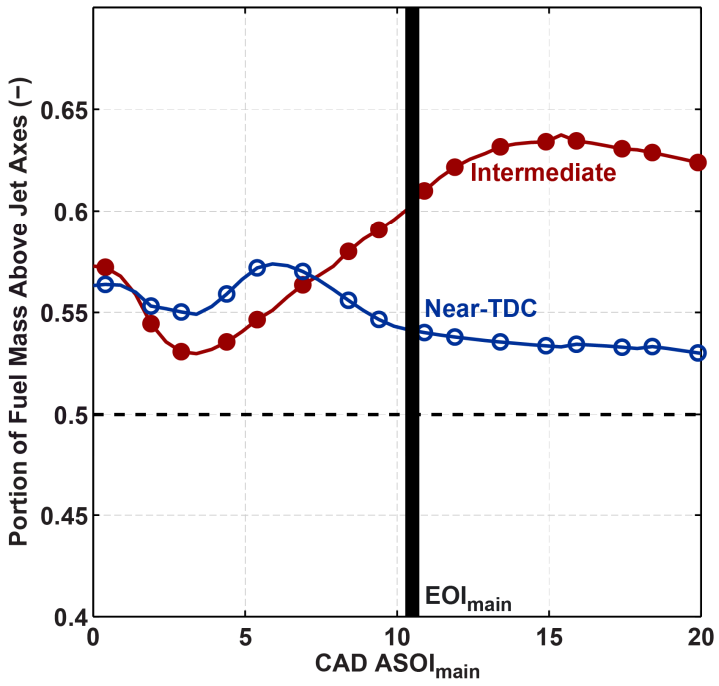

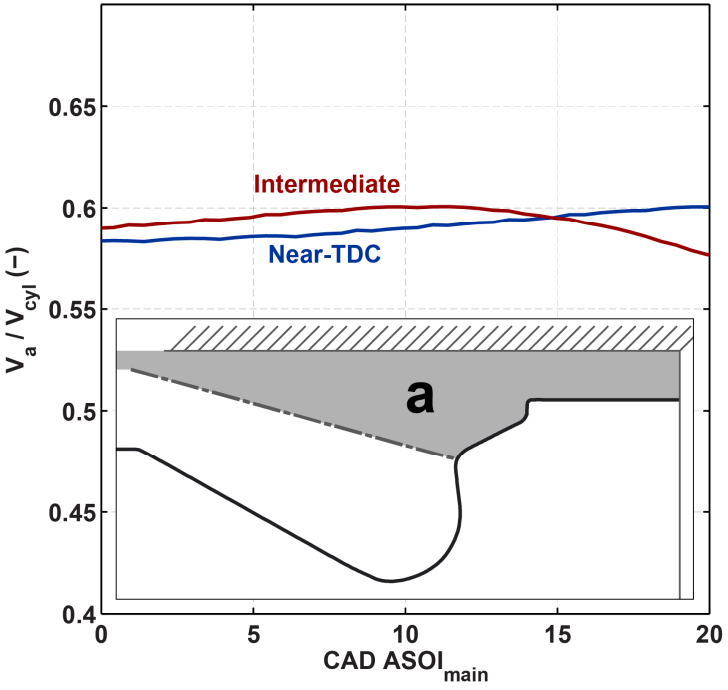

Analysis of spray-bowl interactions – mass and momentum flux calculations

- How do spray-wall interactions affect mass and momentum flux into the upper portion of the chamber?
- Control surface analysis – horizontal plane that moves with the piston top
  - CFD results: plane is defined by faces of a triangulation of computational cells

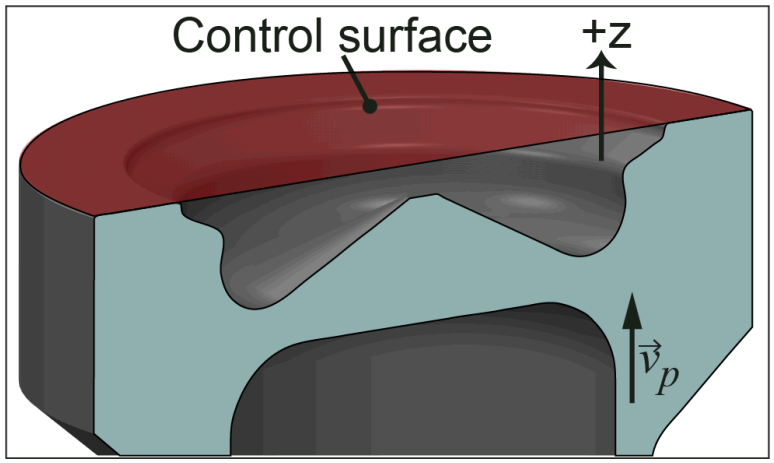

Cross section view

- Mass flux defined for each triangulated face

$$j_m = \rho \left(\vec{v} - \vec{v}_p\right) \cdot \hat{n}$$

- Vertical momentum flux defined for each triangulated face

$$\dot{\varphi}_z = \rho \, v_z \left(\vec{v} - \vec{v}_p\right) \cdot \hat{n}$$

Peak upward mass flux is higher near the step for the intermediate injection timing

- Squish and reverse squish affects the mass flux through the control surface
  - Net mass flux: $j_m - j_{m,motored}$
- For both injection timings, peak vertical mass flux occurs approximately 9 CAD after SOI_{main} (images at right)
- Differences in the chamber center are difficult to interpret; the control surface moves relative to the injector
- Regions of strong upward mass flux appear near the upper bowl rim
  - Greater azimuthal spreading at intermediate injection timing
  - Peak total mass flow nearly 45% larger for intermediate injection timing

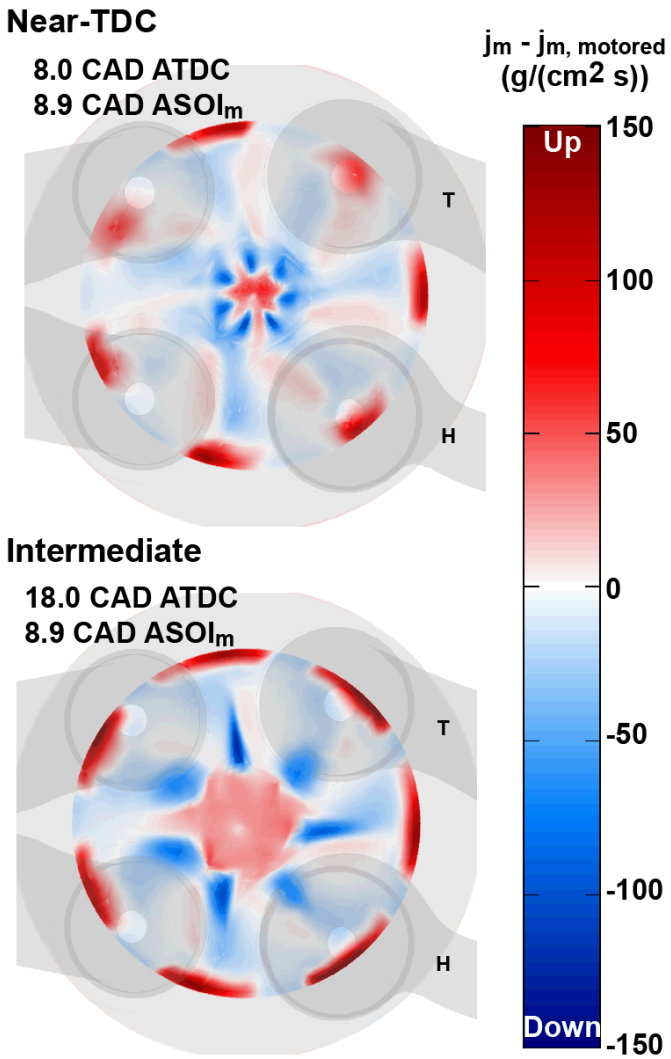

Upward momentum flux at the outer rim is much larger for the intermediate injection timing

- Air entrainment contributes little to the total momentum flux through the control surface
  - Momentum flow through the control surface is dominated by fuel momentum
- Upward momentum flux at the outer rim is larger for the intermediate injection timing
  - Flux is concentrated in narrow segments
- Peak total vertical momentum flow is nearly twice as large for the intermediate injection timing
  - The vertical momentum per unit mass (upward velocity) must also be larger
- More momentum is available as the secondary jets leave the piston surface and penetrate toward the cylinder head

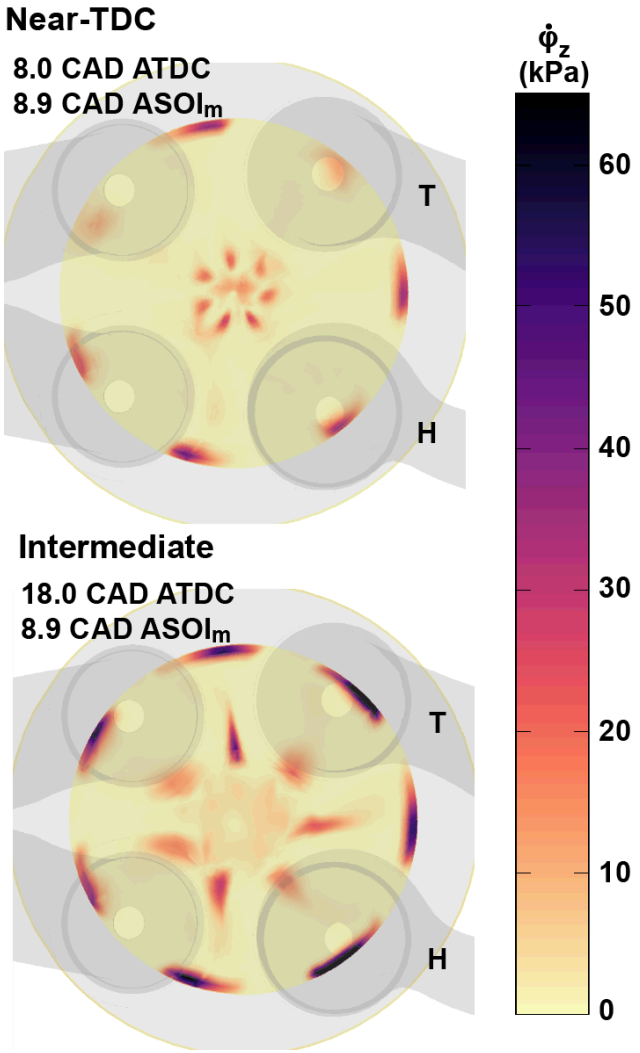

Reverse squish flow aids flow into the squish region, but it this effect is relatively small

- Reverse squish momentum flux is predicted with a 0D model
- Momentum flux peaks near the end of the near-TDC injection, but its magnitude is much smaller than the momentum fluxes associated with the injection jets
  - Reverse squish supports penetration into the squish region, but this effect is relatively small compared to the effects of jet-wall interactions

0D model for average squish flux

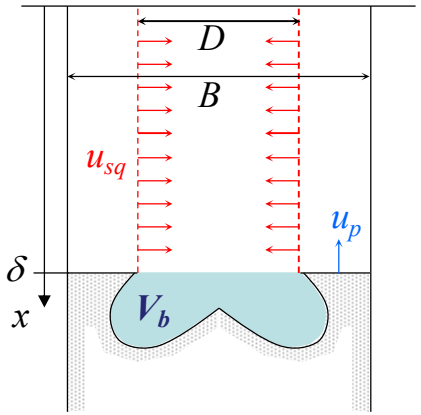

$$u_{sq} = u_p \frac{B^2 - D^2}{D\delta\left(4 + \frac{\pi B^2 \delta}{V_b}\right)}$$

$$\dot{\varphi}_{squish} = \rho u_{sq}(\vec{u}_{sq} \cdot \hat{r})$$

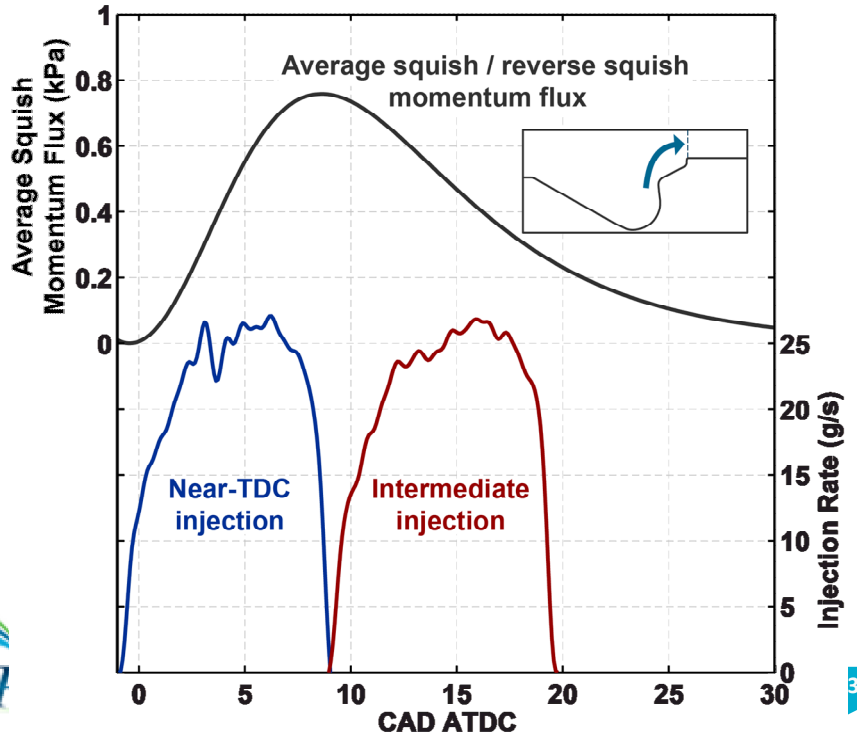

Differences in bulk gas density at different injection timings have a significant impact on penetration velocity

- Bulk gas density is approximately 20% lower for the intermediate injection timing
  - Estimated: 20.5 kg/m³ @ 5 CAD ATDC vs. 16.1 kg/m³ @ 15 CAD ATDC)
- Effect on spreading angle
  - Spreading angle model[1]: $tan\left(\frac{\theta_{inj}}{2}\right) = \frac{2\sqrt{3}\pi}{(3+0.28 l_{noz}/d_{noz})}\sqrt{\frac{\rho_g}{\rho_l}}$
  - Simplified estimate: constant density, neglect effects of combustion
  - Spreading angle: 14.9° for near-TDC injection timing; 13.2° for intermediate injection timing
- Effect on jet penetration velocity
  - Naber and Siebers[2]: $\tilde{t} = \frac{\tilde{S}}{2} + \frac{\tilde{S}}{4}\sqrt{1+16\tilde{S}^2} + \frac{1}{16} ln\left(4\tilde{S} + \sqrt{1+16\tilde{S}^2}\right)$
  - Quasi-steady penetration velocity is 13% faster for the intermediate injection timing

[1]Perini, F. and Reitz, R. D., "Improved atomization, collision and sub-grid scale momentum coupling models for transient vaporizing engine sprays," International Journal of Multiphase Flow, 79(107-123, 2015, DOI: http://doi.org/10.1016/j.ijmultiphaseflow.2015.10.009
[2]Naber, J. D. and Siebers, D. L., "Effects of Gas Density and Vaporization on Penetration and Dispersion of Diesel Sprays," SAE Technical Paper 960034, 1996, DOI: 10.4271/960034

Velocities within the jet are higher for the intermediate injection timing

- Near-TDC injection timing
  - Image shown just after EOI_{main}
  - Velocities in the jet are slower, particularly as it penetrates into the squish region
- Intermediate injection timing
  - Jet appears narrower and penetrates faster
    - Rough estimate: 9-18% higher penetration speed based on time of wall impingement
  - This is consistent with decreasing bulk gas density during the expansion stroke:
    - Decreased air entrainment
    - Higher penetration rate

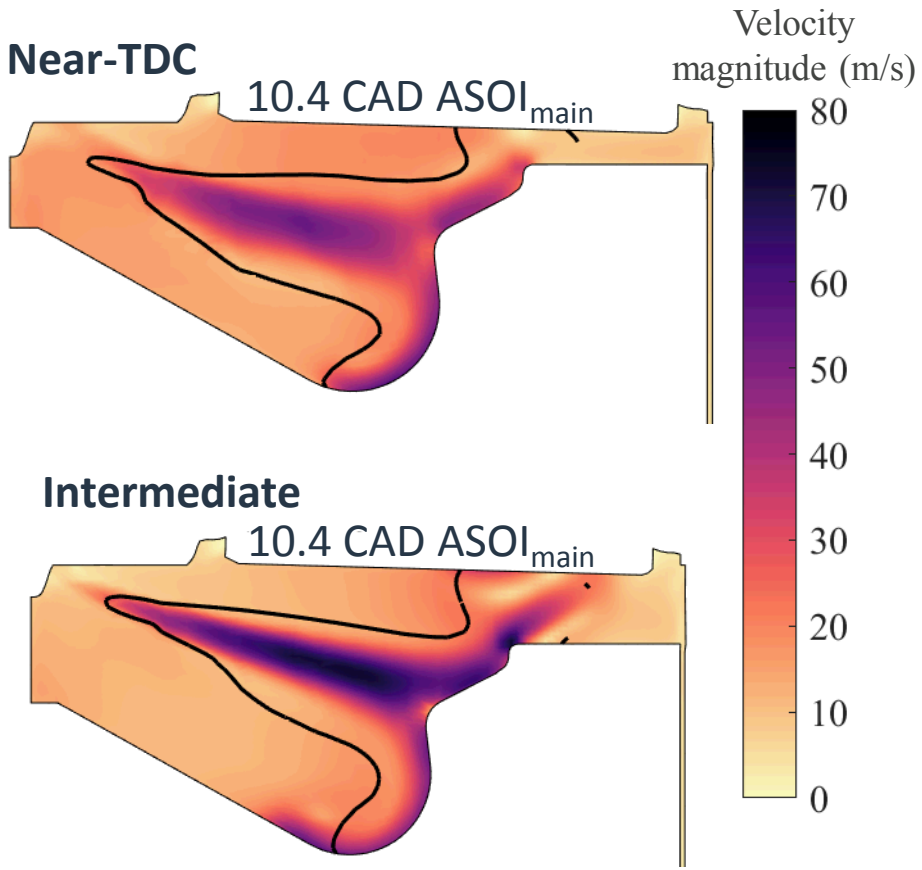

Comparison shortly after end-of-injection; black lines are stoichiometric iso-contour

Radial pressure gradients

- For incompressible, inviscid flows with no body forces, the radial momentum equation for the mean flow is: $\frac{\partial p}{\partial r} = \rho \frac{u_\theta^2}{r} - \rho \frac{Du_r}{Dt}$
  - For solid-body rotation, a radial pressure gradient exists because of $\rho \frac{u_\theta^2}{r}$
  - Squish-swirl interactions and fuel injection contribute to both $\rho \frac{Du_r}{Dt}$ and $\rho \frac{u_\theta^2}{r}$
- Total derivative of radial velocity: $\frac{Du_r}{Dt} = \frac{\partial u_r}{\partial t} + u_r \frac{\partial u_r}{\partial r} + \frac{u_\theta}{r}\frac{\partial u_r}{\partial \theta} + u_z \frac{\partial u_r}{\partial z}$
  - $\frac{\partial u_r}{\partial t}$ is the radial acceleration
  - $\frac{\partial u_r}{\partial t} = \frac{-1}{\rho}\frac{\partial p}{\partial r} + \frac{u_\theta^2}{r} - u_r \frac{\partial u_r}{\partial r} - \frac{u_\theta}{r}\frac{\partial u_r}{\partial \theta} - u_z \frac{\partial u_r}{\partial z}$
- Radial acceleration depends on velocity, so it is normalized by the local velocity magnitude (shown with units of (1/CAD)
  - $\frac{1}{|\vec{u}|}\frac{\partial u_r}{\partial t} = \frac{-1}{\rho|\vec{u}|}\frac{\partial p}{\partial r} + \frac{1}{|\vec{u}|}\frac{u_\theta^2}{r} - \frac{u_r}{|\vec{u}|}\frac{\partial u_r}{\partial r} - \frac{u_\theta}{r|\vec{u}|}\frac{\partial u_r}{\partial \theta} - \frac{u_z}{|\vec{u}|}\frac{\partial u_r}{\partial z}$

Velocity-normalized radial acceleration

$$\frac{\mathbf{1}}{|\vec{u}|}\frac{\partial u_r}{\partial t} = \frac{-1}{\rho|\vec{u}|}\frac{\partial p}{\partial r} + \frac{1}{|\vec{u}|}\frac{u_\theta^2}{r} - \frac{u_r}{|\vec{u}|}\frac{\partial u_r}{\partial r} - \frac{u_\theta}{r|\vec{u}|}\frac{\partial u_r}{\partial \theta} - \frac{u_z}{|\vec{u}|}\frac{\partial u_r}{\partial z}$$

- Initial spray penetration
  - Comparable radial acceleration structure
  - Radial acceleration is stronger near leading edge for intermediate injection timing
- Jet-step interaction
  - Structure is comparable, but develops much faster for the intermediate injection timing
  - Injection of fuel and momentum continues to aid outward penetration for the intermediate injection timing
  - Stronger outward radial acceleration between the piston and the head for the intermediate injection timing – **why?**

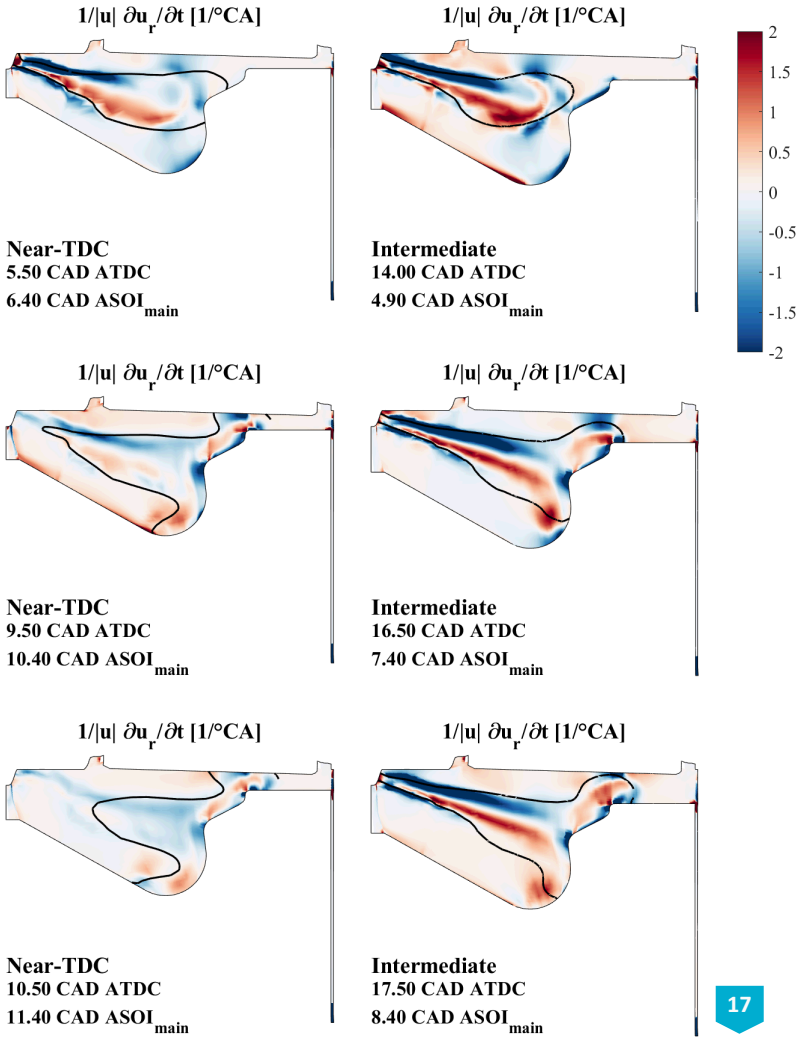

Radial pressure gradient contribution

$$\frac{1}{|\vec{u}|}\frac{\partial u_r}{\partial t} = \frac{-1}{\rho|\vec{u}|}\frac{\partial p}{\partial r} + \frac{1}{|\vec{u}|}\frac{u_\theta^2}{r} - \frac{u_r}{|\vec{u}|}\frac{\partial u_r}{\partial r} - \frac{u_\theta}{r|\vec{u}|}\frac{\partial u_r}{\partial \theta} - \frac{u_z}{|\vec{u}|}\frac{\partial u_r}{\partial z}$$

- Initial spray penetration
  - Comparable pressure gradient distribution
  - Radial pressure gradient is stronger relative to local velocity for the intermediate injection timing
- Jet-step interaction
  - Radial pressure gradient acts to impede outward flow within the jet heads
  - Similar structure for both injection timings, but the structure develops more slowly for the near-TDC injection timing
  - Strong positive accelerations in the squish region are not related to this term

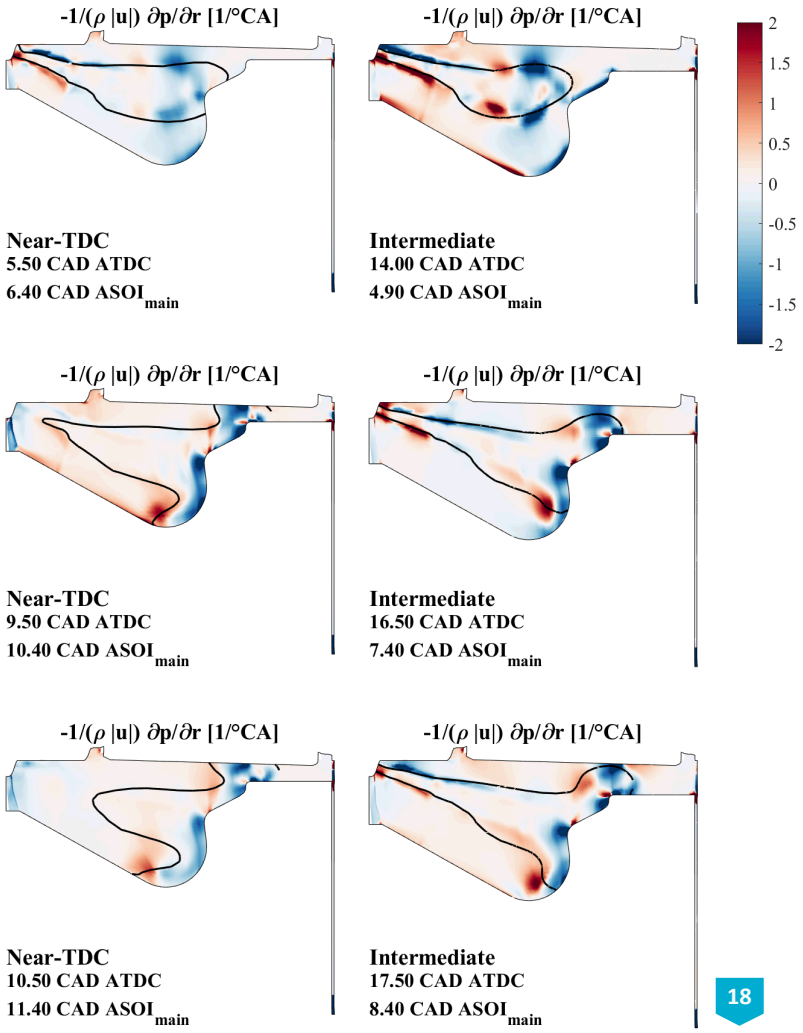

Centrifugal force contribution

$$\frac{1}{|\vec{u}|}\frac{\partial u_r}{\partial t} = \frac{-1}{\rho|\vec{u}|}\frac{\partial p}{\partial r} + \frac{1}{|\vec{u}|}\frac{u_\theta^2}{r} - \frac{u_r}{|\vec{u}|}\frac{\partial u_r}{\partial r} - \frac{u_\theta}{r|\vec{u}|}\frac{\partial u_r}{\partial \theta} - \frac{u_z}{|\vec{u}|}\frac{\partial u_r}{\partial z}$$

- Centrifugal force does not significantly affect radial acceleration
  - The centrifugal force observed near the chamber is attributed to swirl asymmetry and small radii
- What role does swirl play in determining the efficiency/emissions behavior of a stepped-lip piston?

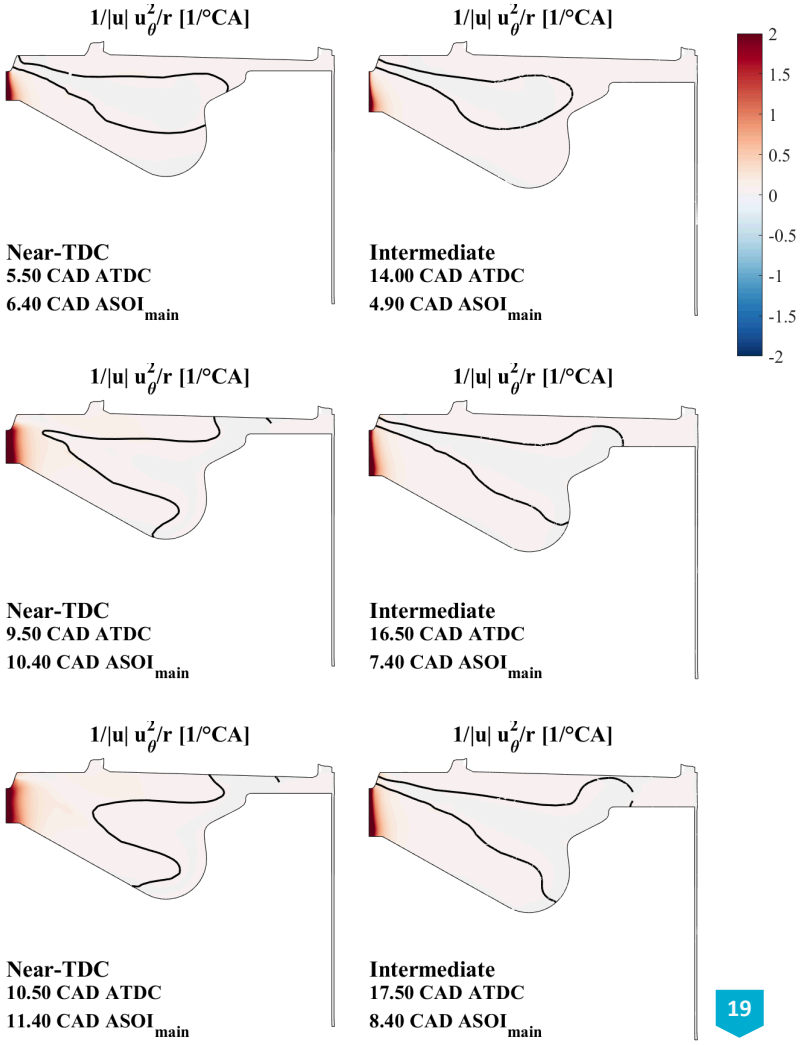

Radial convection contribution

$$\frac{1}{|\vec{u}|}\frac{\partial u_r}{\partial t} = \frac{-1}{\rho|\vec{u}|}\frac{\partial p}{\partial r} + \frac{1}{|\vec{u}|}\frac{u_\theta^2}{r} - \frac{u_r}{|\vec{u}|}\frac{\partial u_r}{\partial r} - \frac{u_\theta}{r|\vec{u}|}\frac{\partial u_r}{\partial \theta} - \frac{u_z}{|\vec{u}|}\frac{\partial u_r}{\partial z}$$

- The radial convection term is also insignificant in determining the radial acceleration

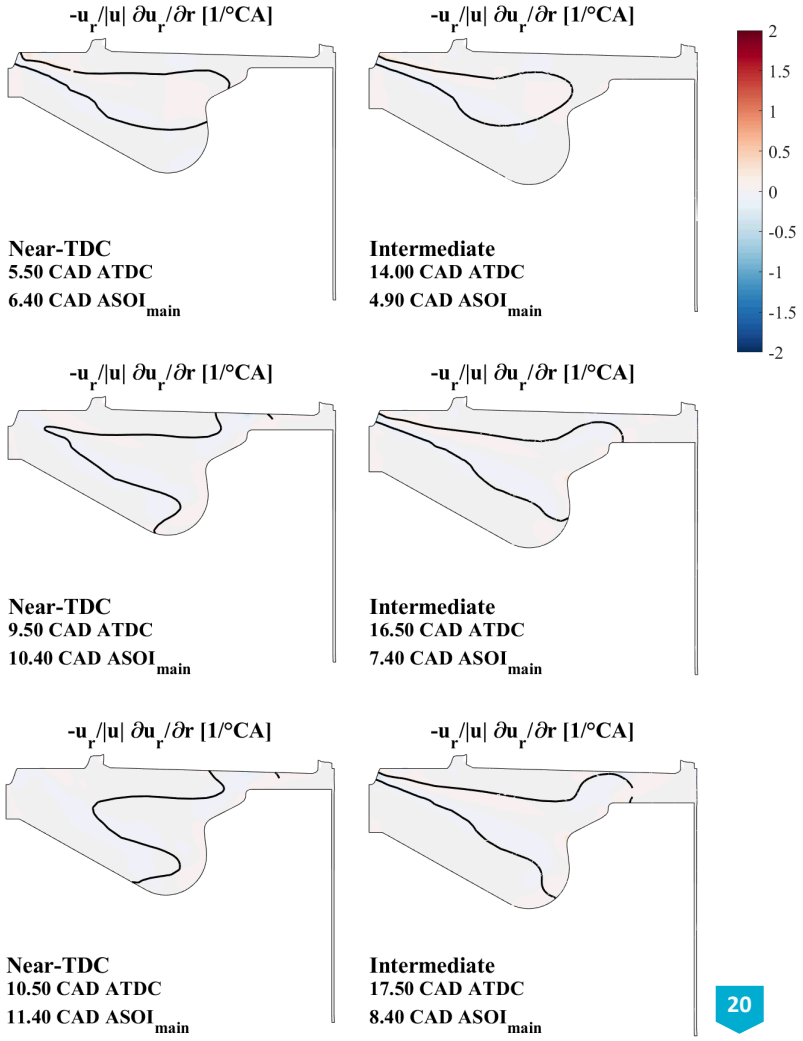

Tangential convection contribution

$$\frac{1}{|\vec{u}|}\frac{\partial u_r}{\partial t} = \frac{-1}{\rho|\vec{u}|}\frac{\partial p}{\partial r} + \frac{1}{|\vec{u}|}\frac{u_\theta^2}{r} - \frac{u_r}{|\vec{u}|}\frac{\partial u_r}{\partial r} - \frac{u_\theta}{r|\vec{u}|}\frac{\partial u_r}{\partial \theta} - \frac{u_z}{|\vec{u}|}\frac{\partial u_r}{\partial z}$$

- Tangential convection seems to play at most a second-order role in determining radial acceleration
  - This term may play a more significant role in other regions of the chamber with substantial tangential spreading due to jet-wall interactions

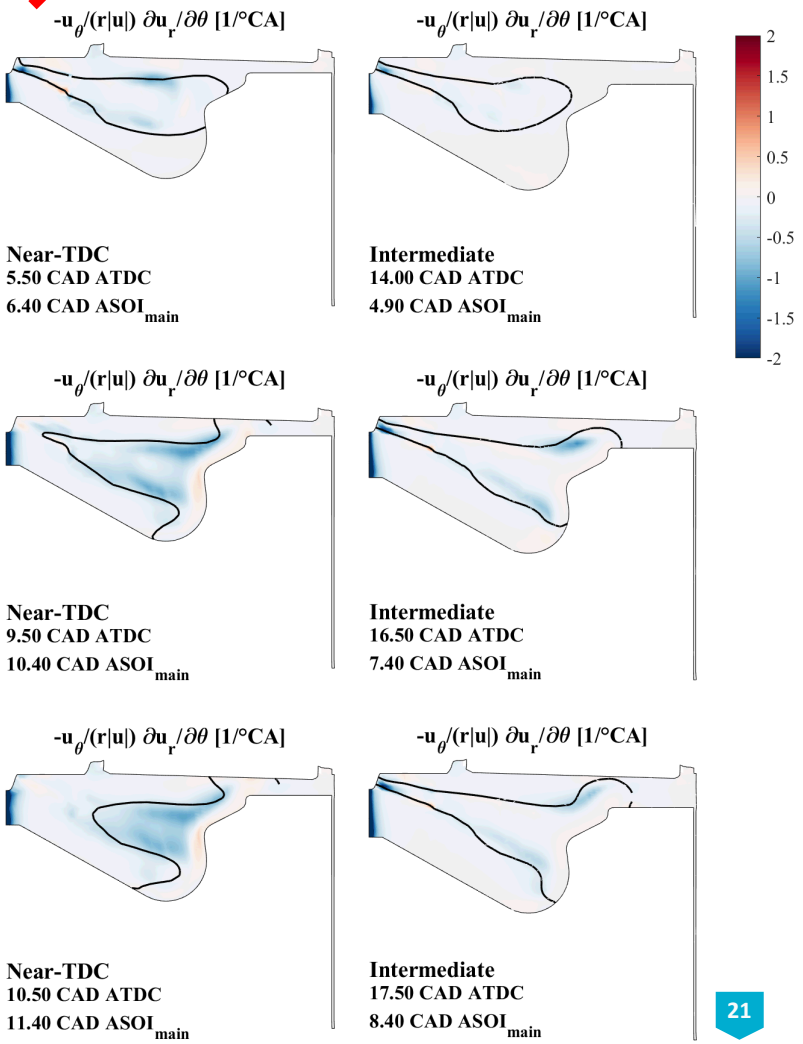

Tangential convection contribution

$$\frac{1}{|\vec{u}|}\frac{\partial u_r}{\partial t} = \frac{-1}{\rho|\vec{u}|}\frac{\partial p}{\partial r} + \frac{1}{|\vec{u}|}\frac{u_\theta^2}{r} - \frac{u_r}{|\vec{u}|}\frac{\partial u_r}{\partial r} - \frac{u_\theta}{r|\vec{u}|}\frac{\partial u_r}{\partial \theta} - \frac{u_z}{|\vec{u}|}\frac{\partial u_r}{\partial z}$$

- Initial spray penetration
  - Similar vertical convection structure
- Jet-step interaction
  - The vertical convective term is responsible for the positive radial acceleration in the squish region
  - $\frac{u_z}{|\vec{u}|}$ is positive where the secondary jet separates from the step surface
  - Injection of fuel and momentum continues to aid outward penetration for the intermediate injection timing

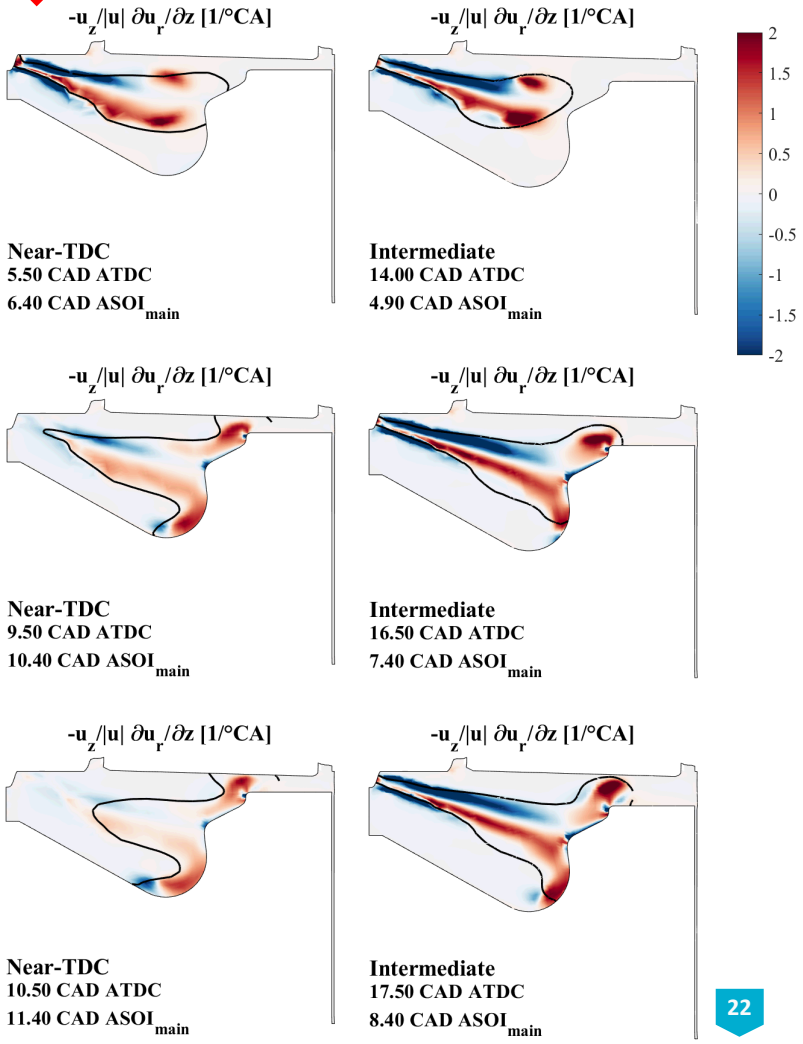

Decomposition of $-\frac{u_z}{|\vec{u}|}\frac{\partial u_r}{\partial z}$

$$\frac{1}{|\vec{u}|}\frac{\partial u_r}{\partial t} = \frac{-1}{\rho|\vec{u}|}\frac{\partial p}{\partial r} + \frac{1}{|\vec{u}|}\frac{u_\theta^2}{r} - \frac{u_r}{|\vec{u}|}\frac{\partial u_r}{\partial r} - \frac{u_\theta}{r|\vec{u}|}\frac{\partial u_r}{\partial \theta} - \boldsymbol{\frac{u_z}{|\vec{u}|}\frac{\partial u_r}{\partial z}}$$

- $\frac{u_z}{|\vec{u}|}$ (top row)
  - Similar structure for both injection timings
- $\frac{\partial u_r}{\partial z}$ (bottom row)
  - The magnitude of this term is greater for the intermediate injection timing throughout the jet and throughout the injection event
  - Negative vertical gradients of radial velocity are the fundamental driver of acceleration into the squish region
  - Vertical gradients of radial velocity appear to scale with injection velocity

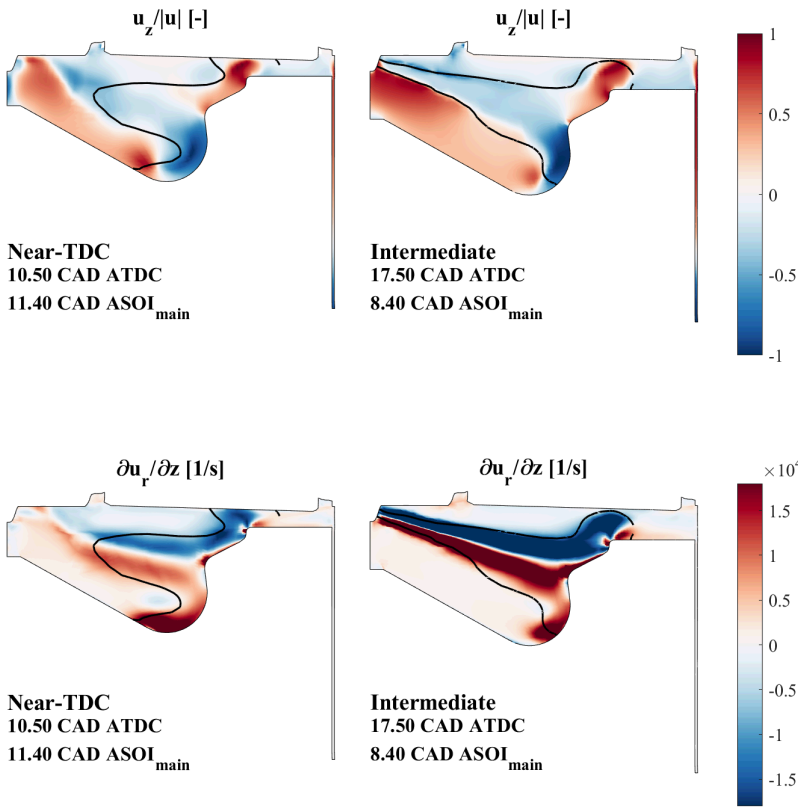

Summary: keys to injection timing impact on turbulent flow evolution

- Effect 1: spray targeting / fuel splitting
  - At the intermediate injection timing, a greater proportion of fuel mass and momentum are deflected upward by the step surface
  - Difference in amount of mass above jet axes: 15% or greater near EOI_{main}

- Effect 2: bulk gas density effect
  - Lower densities at later injection timings lead to faster jet propagation and higher velocities throughout the jet
    - Jet-wall interactions occur before the end of the intermediate injection
    - At the intermediate injection timing, larger vertical gradients of radial velocity more effectively drive flow into the squish region
    - Therefore, higher penetration velocities are theorized to more effectively create beneficial recirculation regions

Next steps in this project

- Injection duration variation: three methods
  - Change injection duration, keep nozzle size and rail pressure constant
  - Change nozzle hole size; keep rail pressure and injected mass constant
  - Change injection pressure; keep nozzle size and injected mass constant

- Combusting results
  - Predictions of efficiency and soot emissions
  - Comparison with velocimetry measurements – can we predict flow structure evolution consistently with experimental data?

- Recommendations for combustion system design

Acknowledgments

- Computational support, simulation post-processing toolbox
  - Federico Perini (UW)

- Technical input and project guidance
  - Alok Warey, Dick Peterson (GM)
  - Eric Kurtz (Ford)

- Laboratory operations assistance
  - Tim Gilbertson (Sandia)

- Financial support: DOE program
  - Gurpreet Singh
  - Leo Breton

Thank you for your attention

Questions?

Turbulent flow structure develops faster with the intermediate injection timing, but doesn't change shape

- Turbulence intensity definition:

$$I = \frac{\sqrt{\frac{1}{3}(u_x'^2 + u_y'^2 + u_z'^2)}}{|\vec{u}|}$$

- The flow structure in the squish region develops a similar structure regardless of injection timing
- Higher jet penetration velocities with the intermediate injection timing establish the flow structure in the squish region sooner
- There does not appear to be a difference in turbulence generation mechanisms in the squish region that changes with injection timing

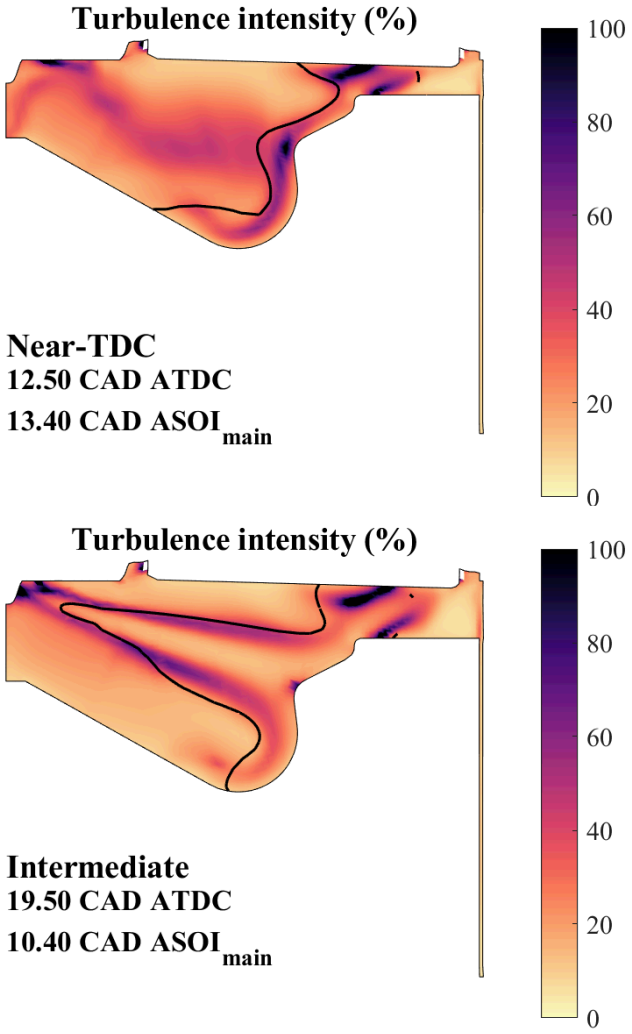

Current spray and turbulence modeling approach in FRESCO

- State-of-the-art spray atomization, droplet collision, and sub-grid scale momentum coupling models have been implemented in FRESCO
- A multi-objective, genetic algorithm-based parameter optimization has been performed based on quantitative ECN data (Spray A)[1]
  - Numerous model constants with complex interactions have been optimized
  - Once optimized, the spray model parameters are not adjusted to provide a true test of the models' predictive capabilities
- A generalized RNG turbulence model has been evaluated for use in these simulations[2]
  - The GRNG model performs adequately for motored in-cylinder flow predictions and very well for jet flow predictions
  - ECN spray A flame structure is well predicted by the GRNG model

[1]Federico Perini, Rolf D. Reitz, Improved atomization, collision and sub-grid scale momentum coupling models for transient vaporizing engine sprays, International Journal of Multiphase Flow, Volume 79, March 2016, Pages 107-123, ISSN 0301-9322, DOI: /10.1016/j.ijmultiphaseflow.2015.10.009

[2]Perini, F., Zha, K., Busch, S. and Reitz, R., "Comparison of Linear, Non-Linear and Generalized RNG-Based k-epsilon Models for Turbulent Diesel Engine Flows," SAE Technical Paper 2017-01-0561, 2017, DOI: 10.4271/2017-01-0561